Preparation and Fluorescence Properties of Poly(*o*-methyl-acrylamideyl-benzoic acid)-ZnS Composites

Qing-Feng Xu, Jian-Mei Lu, Feng Yan, Xue-Wei Xia, Na-Jun Li, Li-Hua Wang, Chun-Hua Ding

Key Laboratory of Organic Synthesis of Jiangsu Province, College of Chemistry, Chemical Engineering and Materials, Soochow University, Suzhou 215123, China

Received 25 February 2009; accepted 8 January 2010
DOI 10.1002/app.32178
Published online 10 June 2010 in Wiley InterScience (www.interscience.wiley.com).

ABSTRACT: Poly(*o*-methyl-acrylamideyl-benzoic acid)-ZnS (P(*o*-MAABA)-ZnS) nanocomposites have been prepared and characterized. The resultant P(*o*-MAABA)-ZnS nanocomposites in solution show two emissions in the purple-light area (370 nm) and in the blue-light area (425 nm), which are assigned to the polymer and ZnS nanoparticles, respectively. The coordination between the polymer and Zn^{2+} and the surface chemical composition has been studied by Infrared spectroscopy and X-ray photoelectron spectroscopy (XPS). The particle size of ZnS nanoparticles was homogeneous and the average size was 3.8 nm, which were characterized by UV absorption spectrum and X-ray Diffraction. The P(*o*-MAABA)-ZnS composites displays good film formability and the films also show two emissions in 370 and 425 nm. After doped with Tb^{3+}, there was effective energy transfer from ZnS nanoparticles to Tb^{3+}. © 2010 Wiley Periodicals, Inc. J Appl Polym Sci 118: 1990–1995, 2010

Key words: poly(*o*-methyl-acrylamideyl-benzoic acid); ZnS nanopartilces; fluorescence

INTRODUCTION

Inorganic nanoparticle/polymer composites are attracting much attention and forming a new branch of materials science.[1–5] According to the literature, inorganic nanoparticle/polymer nanocomposites have been synthesized via sol-gel method,[6–8] intercalation polymerization,[9–11]*in situ* polymerization,[12–14] blend method and ion-changing method.[15,16] However, in case of the sol-gel method, the volatilization of solvent may cause the constriction and brittleness of nanocomposite materials, while it is not easy to control the dispersion of inorganic nanoparticles in the polymer matrix.

These problems may be overcome to some extent by the ion-changing in the polymers prepared by atom transfer radical polymerization (ATRP). ATRP is one of the most effective methods to polymerize a variety of monomers in a controlled fashion, yielding polymers with molecular weights predetermined and with low polydispersities.[17–20] In this system, the protection and limitation of polymers obviously increase the stability of nanoparticles. Besides, the coupling of organic and inorganic components usually results in some composites with novel properties for potential applications.[21]

In this work, poly(*o*-methyl-acrylamideyl-benzoic acid) (P(*o*-MAABA)) with low molecular weight was synthesized via ATRP. Then the P(*o*-MAABA)-ZnS composites were prepared as follows: firstly, Zn^{2+} was distributed in the polymers via the incorporation with carboxy groups and amido groups in P(*o*-MAABA). After the introduction of S^{2-}, ZnS nanoparticles were generated *in situ*. In the composites, the protection and limitation of P(*o*-MAABA) effectively controlled the size and distribution of ZnS in the polymers. The resultant P(*o*-MAABA) -ZnS composites were further doped with Tb^{3+}.

EXPERIMENTAL

Materials and instruments for characterization

Triethylamine (AR, Wulian Chemical Reagent Factory) was distillated in vacuum; Tetrahydrofuran (THF) (AR, Changshu Yangyuan Chemical Reagent Factory) was dried with molecular screen; Copper(I) bromine (CuBr) (AR, Shanghai Zhenxin Chemical Reagent Factory) was dissolved in hydrochloric acid, precipitated into a large amount of deionized water, filtered, washed with ethanol absolute and dried in vacuum. *o*-Aminobenzoic acid (CP, Guoyao chemical Reagent) was used as purchased, other agents were analytic pure and used without any purification.

Correspondence to: J.-M. Lu (lujm@suda.edu.cn).
Contract grant sponsor: Chinese Natural Science Foundation; contract grant numbers: 20476066, 20571054, 20876101.
Contract grant sponsor: Project of Ministy of Education; contract grant number: 20070285003.
Contract grant sponsor: Department of Education Jiangsu Province; contract grant number: 08KJA430004.

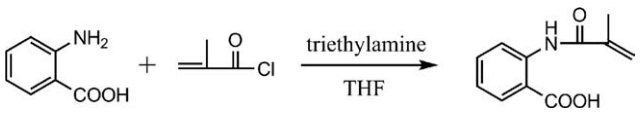

Scheme 1 The synthetic route of o-MAABA.

The ^{1}H-NMR spectra of *o*-MAABA and P(*o*-MAABA) in DMSO-d_6 were measured by Inova 400 MHz FT-NMR spectrometer at ambient temperature. The elementary analysis of *o*-MAABA was obtained using Carlo Erba-MOD1106 elementary analysis instrumentation. Fluorescence spectra were recorded on an Edinburgh-920 fluorescence spectra photometer, excited via the lamp of Xe. Polymer composite films were prepared by spin coating of DMF solution on silex glass via KW-4A desk coating machine. The coated film was dried in a vacuum for 24 h before the characterization. The thickness of the films was controlled in the range of 0.2–0.5 μm, which could be measured using an alpha-step profilometer. UV-visible spectrum was performed by UV-240 spectroscopy. IR analysis was carried out on a Perkin–Elmer 577 IR spectrometer in KBr disks. XRD patterns of the sample was recorded using a RigakuD/max-rA X-ray diffractometer by the use of CuKα irradiation (λ = 1.5418 A) at 40 kV/50 mA with a secondary graphite crystal monochromator. X-ray photoelectron spectroscopy (XPS) measurements were carried out on an ESCALAB MK II system.

Preparation of o-MAABA

As shown in Scheme 1, *o*-Aminobenzoic acid (6.85 g, 0.05 mol) in 50 mL THF was cooled in an ice-bath and triethylamine (10.10 g, 0.1 mmol) was added. The reaction mixture was stirred for 30 min then methyl acryloyl chloride (6.27 g, 0.06 mol) was added via a dropping funnel. The mixture was further stirred for 5 h at room temperature and filtered. The filtrate was neutralized with hydrochloric acid and washed with water. The precipitated *o*-MAABA powder was dried under vacuum.

^{1}H-NMR (400 MHz, DMSO-d_6), δ (ppm): 2.02 (s, 3H), 5.61 (s, 1H), 5.91 (s, 1H), 7.16–7.20 (t, 1H), 7.61–7.65 (m, 1H), 8.02–8.04 (m, 1H), 8.63–8.66 (d, 1H), 11.76 (s, 1H), 13.78 (s, 1H). Anal. Calculation for *o*-MAABA: C, 64.38; H, 5.40; N, 6.83. Found: C, 64.42; H, 5.39; N, 6.85.

Polymerization of o-MAABA

In a three-necked flask, *o*-MAABA (4.10 g), NaOH (0.8 g) and 2,2′-bipyridines (bpy) (0.1872 g) were added with 10 mL DMF and 10 mL de-ionized water, and then stirred. 57.6 mg CuBr and 68 μL EBiB were added to the flask. The flask was cycled between vacuum and N_2 four times and was placed in a 70°C oil bath for 48 h. The mixture was dumped into a large amount of methanol, after neutralized with hydrochloric acid, polymer products were precipitated and filtrated and dried under vacuum.

Preparation of P(o-MAABA)-ZnS and P(o-MAABA)-ZnS:Tb^{3+} composites

P(*o*-MAABA) and $Zn(Ac)_2.2H_2O$ were stirred in water for 72 h at room temperature to obtain P(*o*-MAABA)-Zn, after filtering and washing, the content of Zn in the sample was measured by ICP. P(*o*-MAABA)-Zn and stirred with excessive Na_2S for 48 h at room temperature in de-ionized water, P(*o*-MAABA)-ZnS was obtained after filtering and washing. P(*o*-MAABA)-ZnS was stirred in the $TbCl_3$ solution for 24 h. The resultant powder was filtrated and washed three times with water, P(*o*-MAABA)-ZnS:Tb^{3+} was obtained.

RESULTS AND DISCUSSIONS

Figure 1 shows the ^{1}H-NMR spectrum of P(*o*-MAABA). A broad —CH_2 signal at 3.75 and the disappeared signals at δ = 5.61 ppm and δ = 5.91 ppm which were assigned to the protons of >C=CH_2 in that of monomer indicate the formation of polymer chain.

Figure 2 shows the concentration of Zn^{2+} determined by ICP in the system of P(*o*-MAABA)-Zn. It can be clearly seen that with the increasing of Zn^{2+} used in the preparation, [Zn (wt %) = m(Zn(Ac)$_2$.2H$_2$O)/{m(Zn(Ac)$_2$.2H$_2$O)+m(P(*o*-MAABA))}], the concentration of Zn^{2+} in the P(*o*-MAABA)-Zn system increased until it reached a constant value at about 37%, which arrived the equilibrium value because of the space steric factor of P(*o*-MAABA).

Figure 3 shows the IR spectra of P(*o*-MAABA), P(*o*-MAABA)-Zn and P(*o*-MAABA)-ZnS. After the incorporation of Zn^{2+}, the carbonyl stretching vibration of P(*o*-MAABA) at 1678.17 cm^{-1} shifted to 1659.53 cm^{-1}, the —NH flexural vibration band red-shifted from 1524.25 cm^{-1} to 1509.55 cm^{-1} and the —OH flexural vibration band shifted from 1386.23 cm^{-1} to 1372.55 cm^{-1}. All these results indicate that the amido and carboxyl groups of P(*o*-MAABA) have been coordinated with Zn^{2+}. However, the formation of ZnS weakened the coordination of carbonyl and Zn^{2+}, and the carbonyl stretching vibration blue-shifted to 1667.32 cm^{-1}; —NH flexural vibration and —OH flexural vibration preserved to the original site.

A detailed analysis of chemical composition of P(*o*-MAABA)-ZnS composites was carried out by XPS. The surface scans revealed the presence of zinc, sulfur, oxygen, carbon, and nitrogen (Fig. 4). The C_{1s}

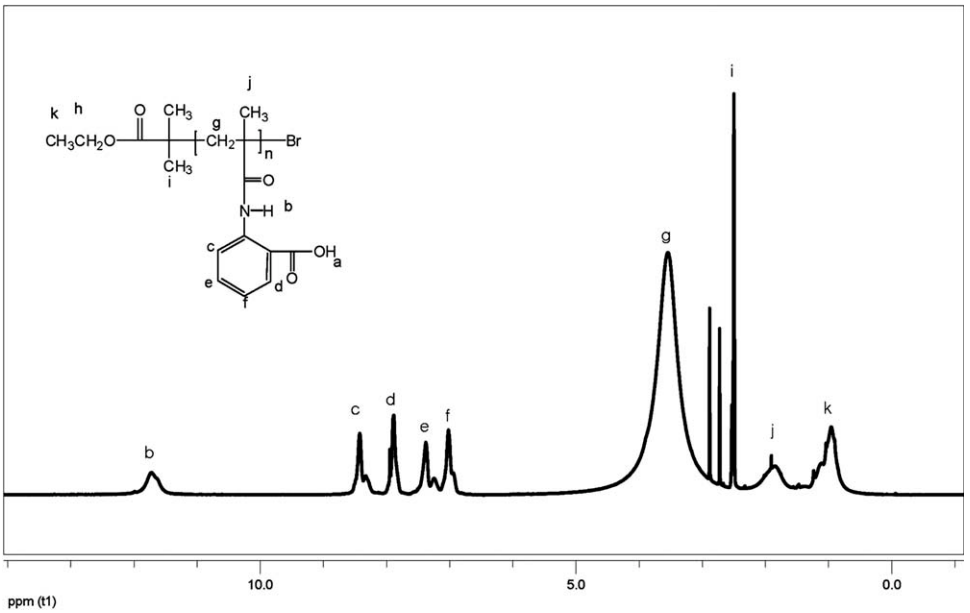

Figure 1 ^{1}H-NMR spectrum of P(*o*-MAABA) with DMSO-d_6 as solvent.

spectra consisted of peaks at 284.8 and 288.1 eV, corresponding to alkyl and carboxylate carbon, respectively. The peak of O_{1s} was at 531.5 eV, which was in agreement with O_{1s} in carboxylate (530.5–531.5 eV) and —OH (531–532 eV). The surface $Zn_{2p3/2}$ component for the composites had a binding energy (BE) of ≈1022.0 eV (full width at half maximum (FWHM) = 2.1 eV). The S_{2p} surface signal was at BE = 161.8 eV (FWHM = 2.0 eV), which was typical of sulfide (S^{2-}) species.[19] According to the results of IR and XPS, we can conclude that the P(*o*-MAABA) has bonded onto the ZnS nanoparticles.

Figure 5 shows the XRD pattern of P(*o*-MAABA)-ZnS. The peaks at 2Θ = 28.8°, 48.0°, and 56.6° assigned to the (111), (220), and (311) planes of cubic crystalline ZnS, respectively. The average crystalline size of ZnS, which was estimated from the half-width of diffraction peaks using the Debye-Scherrer formula, was 3.8 nm. Figure 6 showed the UV absorption spectrum of ZnS in P(*o*-MAABA), the UV absorption blue shifted obviously, which indicated that the effect of restrained quantum increased the band gap of ZnS nanoparticles. According to the effective mass approximation, the relationship of restrained energy of nanoparticles E_c and particle size could be expressed as the following equation[20,21]:

$$E_c = h^2/8\mu R^2 - 1.786e^2/\varepsilon R + (e^2/R)\,\Sigma a_n(S_n/R)^{2n} \quad (1)$$

$1/\mu = 1/m_e + 1/m_h$, μ represents effective mass, εis dielectric constant. The first item of the equation is kinetic energy of confined excition. The second

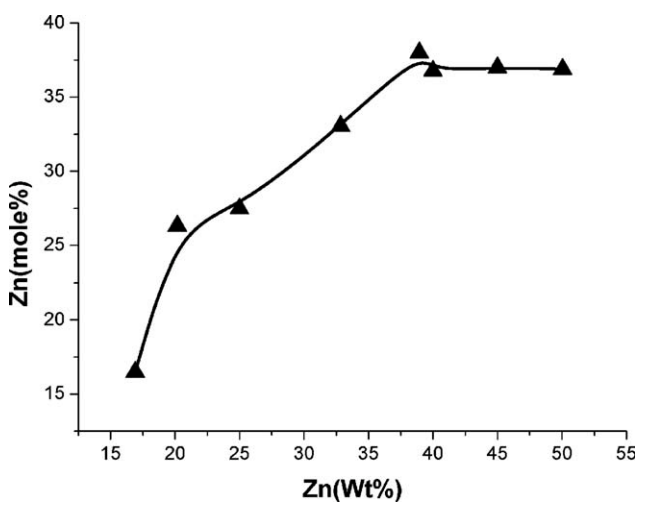

Figure 2 Zn^{2+} concentration (mole%) determined by ICP in P(*o*-MAABA)-Zn.

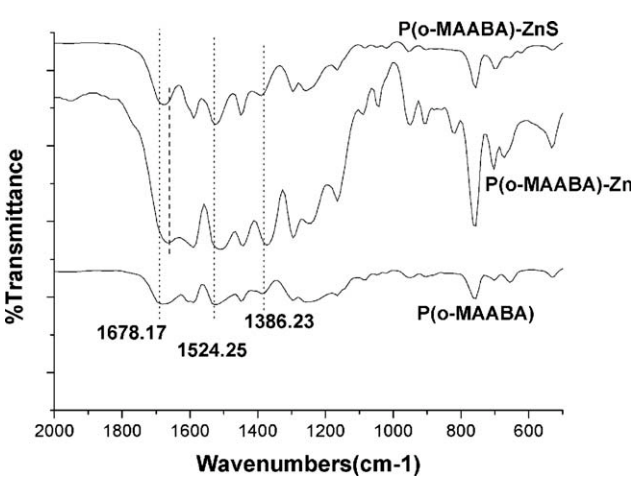

Figure 3 IR spectra of P(*o*-MAABA), P(*o*-MAABA)-Zn and P(*o*-MAABA)-ZnS.

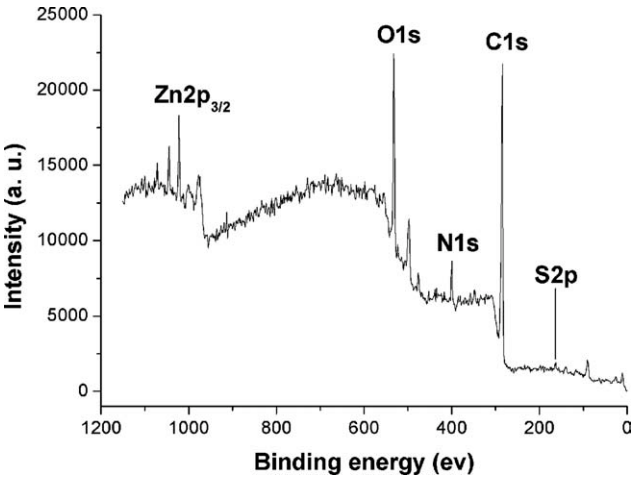

Figure 4 XPS wide-scan spectrum (0-1200 eV) for P(*o*-MAABA)-ZnS composites.

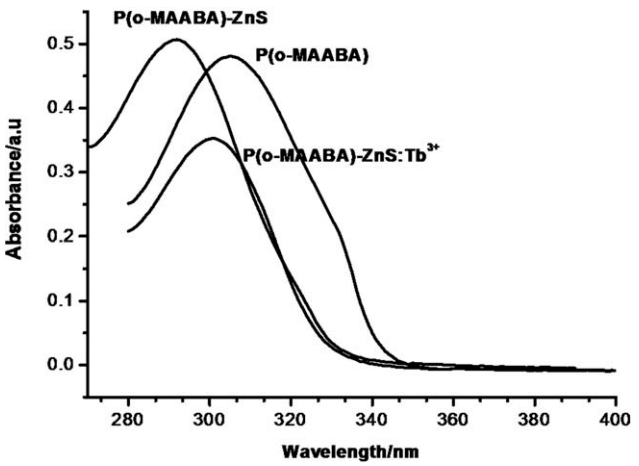

Figure 6 UV spectra of P(*o*-MAABA), P(*o*-MAABA)-ZnS and P(*o*-MAABA)-ZnS:Tb^{3+}.

item is the Coulomb interaction energy of electron and hole. The last item is the correction term of Coulomb interaction energy, which could be ignored. The band-gap energy of bulk ZnS is 3.68 eV,[20] the effective mass is 0.176 m_e, $\varepsilon = 8.3$.[4] The absorption peak of ZnS in P(*o*-MAABA)-ZnS was 290 nm (4.24 eV), blue shifted 0.6 eV from bulk ZnS, and its average particle size calculated form the eq. (1) was 3.8 nm, which in a good agreement with the results from XRD analysis.

According to Figures 7 and 8, P(*o*-MAABA) was seriously aggregated (Fig. 7) while P(*o*-MAABA)-ZnS particles were distinct and could be distinguished (Fig. 8). These results confirmed that the phenomena of nanoparticles agglomeration were decreased effectively because the nanoparticles cores were kept apart by the interaction between polymer and nanoparticles. P(*o*-MAABA) effectively controlled the size of ZnS nanoparticles, modified the surface of nanoparticles and made them stable, which caused the uniformity of P(*o*-MAABA)-ZnS composites.

Fluorescence property of P(o-MAABA)-ZnS nanocomposite

Figure 9 shows the emission spectra of P(*o*-MAABA) and P(*o*-MAABA)-ZnS in DMF solution. When the excitation wavelength was 314 nm, the emission peak of P(*o*-MAABA) was at 370 nm while two emission peaks at 370 and 425 nm were observed in P(*o*-MAABA)-ZnS nanocomposite. The emission peak at 370 nm was assigned to P(*o*-MAABA), and the emission peak at 425 nm was the self-activation emission peak of ZnS nanoparticles.

Figure 10 shows the emission spectra of P(*o*-MAABA)-ZnS nanocomposite film. When the excitation wavelength was 314 nm, two emission peaks at 370 and 425 nm were observed in P(*o*-MAABA)-ZnS nanocomposite film. Same as in DMF solution, the

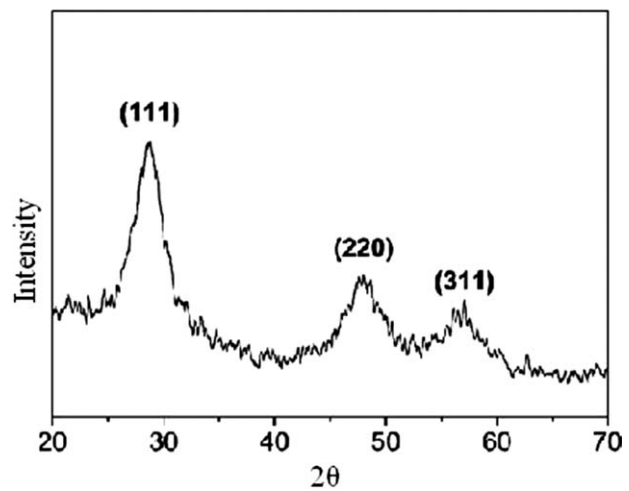

Figure 5 XRD pattern of P(*o*-MAABA)-ZnS.

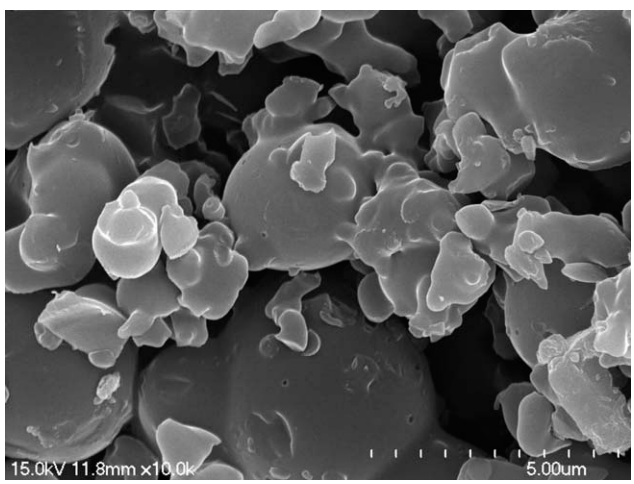

Figure 7 SEM images of P(*o*-MAABA).

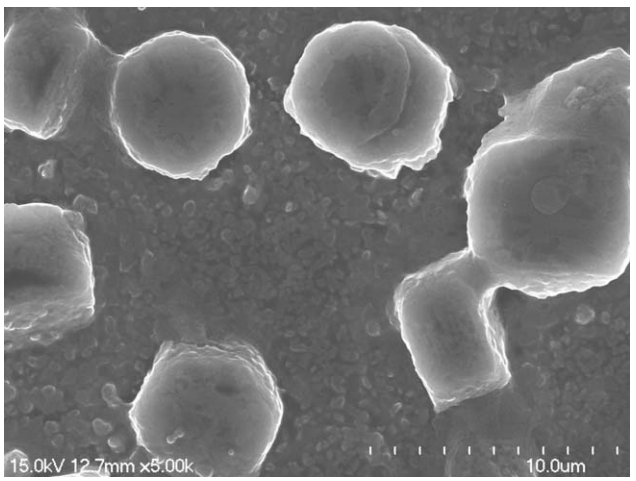

Figure 8 SEM images of P(*o*-MAABA)-ZnS.

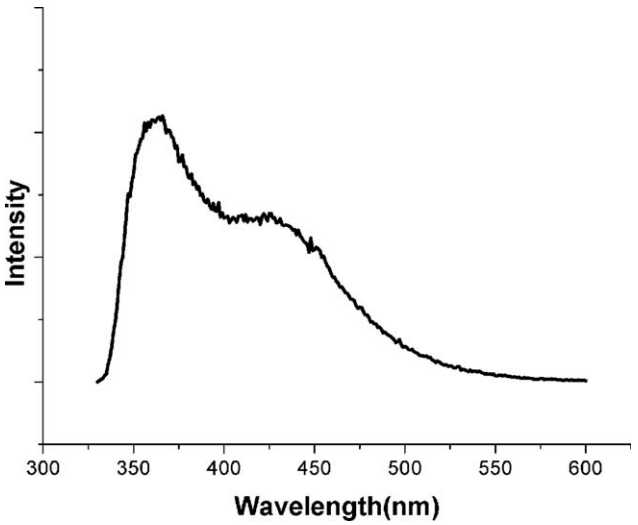

Figure 10 Emission spectra for films of P(*o*-MAABA)-ZnS composite.

emission peak at 370 nm was assigned to P(*o*-MAABA) and the emission peak at 425 nm was the emission peak of ZnS nanoparticles in the film. Film formation did not change the shape, size and distribution of ZnS nanoparticles in the polymers. With the formation of ZnS nanoparticles, the emission of the system changed from monochromatic light to two-tone color lights, which adjusted the emission spectra. Because of good film formability, this composite system may have application in optical devices.

Figure 11 shows the emission spectra of P(*o*-MAABA)-ZnS:Tb^{3+} composites and $TbCl_3$ with the same concentration. Five emission peaks were observed at 370, 490, 545, 585, and 620 nm. As before, the emission peaks at 370 nm was assigned to P(*o*-MAABA), and the emission peaks at 490, 545, 585, and 620 nm were assigned to the $^5D_4$-^7F_J ($J = 6$, 5, 4, 3) transition of Tb^{3+}, and the emission intensity at 545 nm was the highest. As showed in Figure 9, the emission intensity of Tb^{3+} in P(*o*-MAABA)-ZnS:Tb^{3+} composites was higher than in pure $TbCl_3$ with the same concentration, and the emission peak at 425 nm assigned to ZnS nanoparticles disappeared. The two results indicated that there was energy transfer from ZnS nanoparticles to Tb^{3+} in P(*o*-MAABA)-ZnS:Tb^{3+} composites. In addition, the UV-vis absorption spectra of P(*o*-MAABA)-ZnS:Tb^{3+} as shown in Figure 6 also verify the energy transfer between P(*o*-MAABA)-ZnS and Tb^{3+} ion, because the maximum absorption wavelength is red-shifted about 10 nm after addition of Tb^{3+} ion into P(*o*-MAABA)-ZnS composite. It's probably ascribed to the weak interaction of Tb^{3+} ion and the amido bond of P(*o*-MAABA).

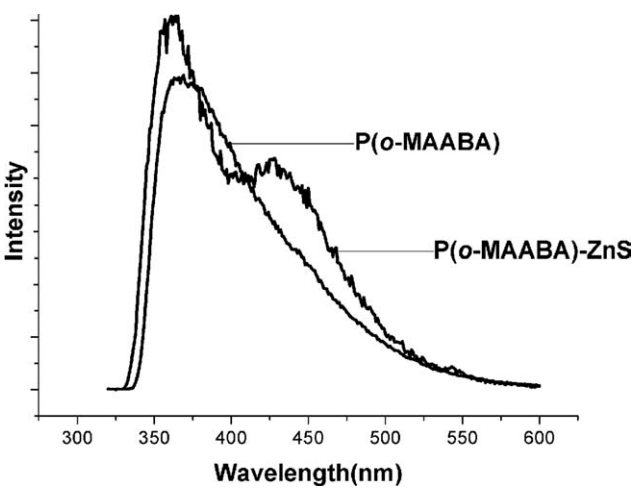

Figure 9 Emission spectra of P(*o*-MAABA) and P(*o*-MAABA)-ZnS (10 mg/10 mL DMF).

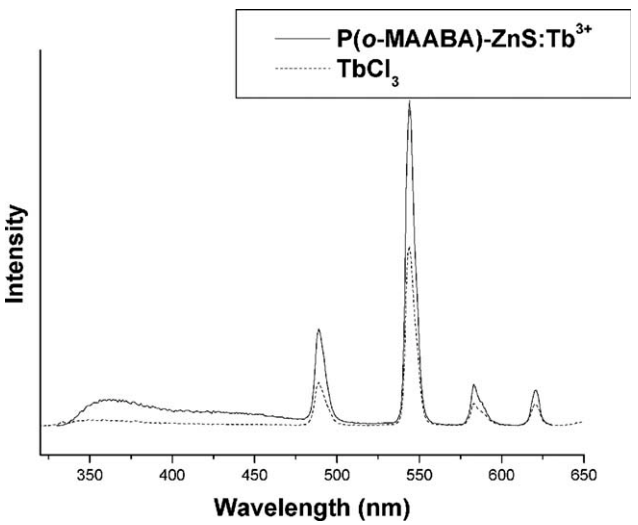

Figure 11 Emission spectra of P(*o*-MAABA)-ZnS:Tb^{3+} and $TbCl_3$ with the same concentration.

CONCLUSION

In this work, P(*o*-MAABA)-ZnS composite has been successfully synthesized. XPS and IR spectra acknowledged the coordination of P(*o*-MAABA) and Zn^{2+}; the average particle size of ZnS estimated from effective mass approximation was 3.8 nm, which was in a good agreement with XRD analysis. The polymers could effectively control particle size of ZnS nanoparticles, modify the surface and stabilize the nanoparticles. The composite system of P(*o*-MAABA)-ZnS expressed unique properties, such as unusual luminescence properties and good film formability. The emission spectra of P(*o*-MAABA)-ZnS (in solutions and films) composed from two peaks: the emission of polymers at 370 nm and the emission of ZnS nanoparticles at 425 nm. When doped with Tb^{3+}, there was energy transfer from ZnS nanoparticles to Tb^{3+}, intense green luminescence was observed in P(*o*-MAABA)-ZnS:Tb^{3+} composites.

References

1. Shimmin, R. G.; Schoch, A. B.; Braun, P. V. Langmuir 2004, 20, 5613.
2. Nakashima, H.; Furukawa, K.; Ajito, K.; Kashimura, Y.; Torimitsu, K. Langmuir 2005, 21, 511.
3. Porel, S.; Singh, S.; Harsha, S. S.; Rao, D. N.; Radhakrishnan, T. P. Chem Mater 2005, 17, 9.
4. Ali, H. A.; Iliadis, A. A. Thin Solid Films 2005, 471, 154.
5. Zhang, H.; Wang, R. B.; Zhang, G.; Yang, B. Thin Solid Films 2003, 429, 167.
6. Chiang, C. L.; Ma, C. C. Eur Polym J 2002, 38, 2219.
7. Jitianu, A.; Garther, M.; Zaharescu, M.; Cristea, D.; Manea, E. Mater Sci Eng 2003, 23, 301.
8. Mokari, T.; Sertchook, H.; Aharoni, A.; Ebenstein, Y.; Avnir, D.; Banin, U. Chem Mater 2005, 17, 258.
9. Anouk, G.; Brocorens, P.; Siri, D.; Gardebien, F.; Bredas, J. L.; Lazzaroni, R. Langmuir 2003, 19, 8287.
10. Kim, B. H.; Jung, J. H.; Hong, S. H.; Joo, J. Macromolecules 2002, 35, 1419.
11. Sun, T.; Juan, M. G. Adv Mater 2002, 14, 128.
12. He, J.; Shen, Y. B.; Yang, J.; Evans, D. G.; Duan, X. Chem Mater 2003, 15, 3894.
13. Xia, H. S.; Wang, Q.; Qiu, G. H. Chem Mater 2003, 15, 3879.
14. Viswanathan, G.; Chakrapani, N.; Yang, H.; Wei, B. Q.; Chung, H.; Cho, K.; Chang, Y. R.; Ajayan, P. M. J Am Chem Soc 2003, 125, 9258.
15. He, J. H.; Kunatake, T.; Nakao, A. Chem Mater 2003, 15, 4401.
16. Abdullah, M.; Lenggoro, I. W.; Okuyama, K.; Shi, F. G. J Phys Chem B 2003, 107, 1957.
17. Tang, H. D.; Tang, J. B.; Ding, S. J.; Maciej, R.; Shen, Y. Q. J Polym Sci Part A: Chem 2005, 43, 1432.
18. Zhang, H. Q.; Jiang, X. L.; Rob Van Der, L. Polymer 2004, 45, 1455.
19. Lutz, J. F.; Börner, H. G.; Weichenhan, K. Macromol Rapid Commun 2005, 26, 514.
20. Xu, F. J.; Kang, E. T.; Neoh, K. G. Macromolecules 2005, 38, 1573.
21. Sun, L. D.; Xu, B.; Fu, X. F.; Wang, M. W.; Qian, C.; Liao, C. S.; Yan, C. H. Sci Cha (Series B) 2001, 31, 146.